Extrathermodynamic Study of Surface Diffusion in Reversed-Phase Liquid Chromatography with Silica Gels Bonded with Alkyl Ligands of Different Chain Lengths

Kanji Miyabe

Faculty of Engineering, Toyama University, 3190, Gofuku, Toyama 930-8555, Japan

Georges Guiochon*

Department of Chemistry, The University of Tennessee, Knoxville, Tennessee 37996-1600, and Division of Chemical Sciences, Oak Ridge National Laboratory, Oak Ridge, Tennessee 37831

Received: January 19, 2005; In Final Form: April 18, 2005

Surface diffusion on adsorbents made of silica gels bonded to C_1, C_4, C_8, and C_{18} alkyl ligands was studied in reversed-phase liquid chromatography (RPLC) from the viewpoints of two extrathermodynamic relationships: enthalpy−entropy compensation (EEC) and linear free-energy relationship (LFER). First, the values of the surface diffusion coefficient (D_s), normalized by the density of the alkyl ligands, were analyzed with the modified Arrhenius equation, following the four approaches proposed in earlier research. This showed that an actual EEC resulting from substantial physicochemical effects occurs for surface diffusion and suggested a mechanistic similarity of molecular migration by surface diffusion, irrespective of the alkyl chain length. Second, a new model based on EEC was derived to explain the LFER between the logarithms of D_s measured under different RPLC conditions. This showed that the changes of free energy, enthalpy, and entropy of surface diffusion are linearly correlated with the carbon number in the alkyl ligands of the bonded phases and that the contribution of the C_{18} ligand to the changes of the thermodynamic parameters corresponds to that of the C_{10} ligand. The new LFER model correlates the slope and intercept of the LFER to the compensation temperatures derived from the EEC analyses and to several parameters characterizing the molecular contributions to the changes in enthalpy and entropy. Finally, the new model was used to estimate D_s under various RPLC conditions. The values of D_s that were estimated from only two original experimental D_s data were in agreement with corresponding experimental D_s values, with relative errors of ∼20%, irrespective of some RPLC conditions.

Introduction

Reversed-phase liquid chromatography (RPLC) is one of the most effective separation techniques available for both analytical and preparative purposes.[1] The abundance of stationary phases that have different physical and chemical properties is one of the essential reasons why RPLC is used in an extremely wide field of chemistry. Although many types of separation media can be used as stationary phases for RPLC, alkyl-ligand-bonded silica gels (and, particularly, C_{18}-silica gels) are still the most popular packing materials for RPLC.[2] It is well-known that the chromatographic behavior of these materials is dependent on the alkyl chain length, the density of these ligands, and the nature of the end-capping treatment of the residual silanol groups. In some cases, chemists attempted to take advantage of the difference in chromatographic behavior of RPLC packing materials bonded with alkyl ligands of different chain lengths and to control the modification conditions of the alkyl ligands intentionally, to achieve specific separations. Many studies have examined the influence of the alkyl chain length on the chromatographic behavior, but mainly from the viewpoint of the retention equilibrium.[3−8] They attempt to clarify the dependence of the retention and separation factors on the carbon content of the material and on the length of the chains bonded to the silica gel. In contrast with these extensive studies on the influence of the alkyl chain length on the retention behavior in RPLC, there are few fundamental studies discussing the dependence of the mass-transfer kinetics on the surface modification conditions of the alkyl ligands bonded to the base silica gel.[9,10]

Under linear conditions, band broadening is dependent on the mass-transfer kinetics of several rate processes involved in chromatography, axial dispersion, external (fluid-to-particle) mass transfer, intraparticle diffusion, and adsorption/desorption kinetics.[11,12] Intraparticle diffusion is usually assumed to consist of two distinct mechanisms: pore diffusion and surface diffusion.[13,14] Surface diffusion has an important role in intraparticle diffusion.[11,12] The manner of surface diffusion is dependent on the retention behavior of the sample molecules, because these molecules migrate on the stationary phase surface, in the adsorbed state. In principle, chromatographic separations are based on the difference between the adsorptive interactions of the sample components with the stationary phase surface. Therefore, surface diffusion should be related to some essential characteristics of chromatographic retention. It is expected that important information about the chromatographic mechanisms in RPLC can be derived from detailed analyses of surface-diffusion phenomena from the viewpoints of the retention equilibrium, the mass-transfer kinetics, the thermodynamics, and the extrathermodynamics. However, few studies besides our own[11,12,15−19] have involved the thermodynamics and extrathermodynamics of surface diffusion in RPLC.

Enthalpy−entropy compensation (EEC) is one of the important extrathermodynamic relationships. It has been applied to many different chemical equilibria and kinetic processes, to

10.1021/jp058028q CCC: $30.25
Published on Web 05/27/2005

TABLE 1: Physicochemical Properties of Reversed-Phase Stationary Phases in Various Main Alkyl Chains

main alkyl chain	C_1	C_4	C_8	C_{18}
particle density, ρ_p (g/cm^3)	0.74	0.73	0.74	0.86
porosity, ϵ_p	0.62	0.61	0.56	0.46
tortuosity factor, k_t	3.9	4.1	4.9	4.5
carbon content (wt %)				
before end-capping	4.1	6.7	9.9	17.1
after end-capping	—[a]	—[a]	—[a]	17.1
ligand density (μmol/m^2)[b]	4.4	3.6	3.3	3.2
average distance between two ligands (nm)[b]	0.69	0.76	0.80	0.81
reaction ratio of silanol group (%)[b]	55	45	42	40
mass of adsorbent in the column (g)	1.8	1.8	1.8	2.1
column void fraction, ϵ_e	0.44	0.42	0.42	0.42
lot number of the adsorbent	EC08937	BE21037	CE21037	DE16037

[a] No end-capping treatment was made. [b] Calculated from the carbon content before end-capping, the BET surface area of the base silica gel (290 m^2/g), and the density of silanol groups on the surface of the base silica gel (assumed to be 8 μmol/m^2).

discuss their reaction mechanisms.[20−24] The establishment of such a compensation has also been supported on some theoretical bases.[25−29] The EEC behavior was also studied for the retention equilibrium in some liquid chromatographic systems, in RPLC,[17−19,30−33] normal-phase liquid chromatography (LC),[34] ion-pair RPLC,[35,36] and ion-exchange LC.[37] In contrast with the large number of studies discussing EEC relationships dealing with retention equilibrium, very few papers have been devoted to EEC relationships that involve surface diffusion, as described previously.

Linear free energy relationships (LFERs) are the other type of extrathermodynamic relationships. The free-energy change (ΔG) of a chemical equilibrium is linearly correlated with that of a related kinetic process or another reaction equilibria. EEC and LFER are empirical extrathermodynamic correlations of thermodynamic quantities that have been used to demonstrate the similarity of the mechanisms of equilibrium or of kinetic processes and to study the characteristics of these processes from the viewpoints of molecular structural contributions. Regarding the thermodynamic and extrathermodynamic properties of RPLC, we have demonstrated actual EEC relationships for the retention equilibrium[17−19,33] and surface diffusion[18,19] in several RPLC systems. We also reported that LFER is observed between the retention equilibrium and surface diffusion in RPLC, irrespective of the experimental conditions, such as the type of sample compounds, the type and composition of the organic modifiers in the mobile phase, the alkyl chain length of bonded ligands on the stationary phase, and the temperature.[11,12,16−19]

Previously,[11,38,39] we studied the influence of the length and density of alkyl ligands on some RPLC characteristics, from the viewpoints of the retention equilibrium, surface diffusion, and their thermodynamic properties. With increasing length of the alkyl chain and density of a C_{18} ligand, the adsorption equilibrium constant (K), the absolute value of the isosteric heat of adsorption (Q_{st}), and the activation energy of surface diffusion (E_s) increase while the value of D_s decreases. There is a critical level of carbon content of the stationary phase above which the last four parameters do not change significantly with increasing alkyl chain length or ligand density. However, we have not yet been able to interpret the dependence of the D_s values on the modification conditions of a base silica gel by alkyl ligands.

This work examines the characteristics and the mechanism of surface diffusion in RPLC systems made with silica gels bonded to different alkyl ligands (C_1, C_4, C_8, and C_{18}). First, we analyzed series of experimental data of D_s from different thermodynamic points of view and studied the decrease of the rate of molecular migration by surface diffusion with increasing retention strength. We derived the activation energy and the frequency factor (D_{s0}) of surface diffusion from the temperature dependence of D_s and studied the linear correlation between ln D_{s0} and E_s. We introduced a new coefficient, δ_s; this parameter is the coefficient D_s normalized by the alkyl ligand density (σ), which is an important factor because σ is dependent on the chain length of the alkyl ligands and searched for an EEC relationship observed for surface diffusion, following the four methods proposed by Krug and co-workers.[25−27] The chain density or coverage of the surface (σ) is defined as the number of moles of alkyl ligand per unit surface area of the base silica gel and is given in units of mol/m^2, as described in the list of symbols. Finally, we derived a new model to account for the influence of several experimental parameters on surface diffusion in RPLC and showed its usefulness for a comprehensive interpretation of the variations of D_s with the experimental conditions of RPLC.

Experimental Section

Columns and Reagents. Table 1 lists the main physicochemical properties of the four packing materials used, which were custom-made items, by special order, purchased from YMC (Kyoto, Japan). The columns (6 mm ID × 150 mm) were packed with the separation media. They are not commercially available. Some of the information in Table 1 were obtained from the manufacturer. The packing materials were probably synthesized by chemically bonding different *n*-alkyldimethylsilyl ligands onto the surface of the same base silica gel. No end-capping treatment was performed for the silica gels bonded with C_1, C_4, and C_8 alkyl ligands. Regarding the C_{18}-silica gel, no substantial increase in the carbon content was observed upon end-capping with the trimethylsilyl ligand. The bonding density of the ligands decreases with increasing bulkiness of the main alkyl chain. The average distance between two ligands increases with increasing length of the main alkyl chain. The average particle diameter of the base silica gel is 45 μm. As described later, this coarse base material was used to make it easier to analyze band broadening phenomena quantitatively and, more specifically, to estimate more-accurate values of D_s from the experimental chromatographic peak profiles.

The mobile phase was a methanol/water mixture (70/30, v/v). Alkylbenzenes (ethylbenzene, *n*-butylbenzene, and *n*-hexylbenzene) were used as the sample compounds. They were all reagent grade and used without further purification. Sample solutions were prepared by dissolving the sample compounds into the mobile phase. The concentration of the sample solutions was 0.1 wt % in most cases. Uracil and sodium nitrate were used as inert tracers to determine the internal porosity (ϵ_p) of the packing materials and the void fraction (external porosity, ϵ_e) of the columns.[2,40,41] The internal porosity is the ratio of the

intraparticulate pore volume to the volume of the stationary-phase particles. The external porosity is the interparticle volume in the column divided by the column volume. Roughly speaking, the pulse elution time of uracil provides the sum of ϵ_p and ϵ_e, whereas that of sodium nitrate provides ϵ_e because of the Donnan salt-exclusion effect.[41] The difference in the elution times of the two inert tracers gives ϵ_p.

Apparatus. A high-performance liquid chromatography (HPLC) system (Model LC-6A, Shimadzu, Kyoto, Japan) was used. A small volume of the sample solution (ca. 0.5 $\sim$ 300 μL) was introduced into the mobile phase stream, using a valve injector (Model 7125, Rheodyne, Cotati, CA). The column temperature was kept at constant levels by circulating temperature-controlled water around the column. The concentration of the sample compound leaving from the column was monitored with an ultraviolet detector of the HPLC system (Model SPD-6A).

Procedure. Pulse response experiments (i.e., elution chromatography) were conducted under different RPLC conditions, with a column temperature between 288 K and 308 K and a volume flow rate of the mobile phase in the range of 1$-$2 cm^3/min. A small concentration pulse or perturbation was introduced into the mobile phase stream at the inlet of the column. In this study, we measured the chromatographic data under conditions of the linear adsorption isotherm of the sample compounds because the amounts that were injected were small enough. The first absolute moment (μ_1) and the second central moment (μ_2') of the elution peaks were analyzed by the moment method. The information regarding the retention equilibrium and the mass-transfer kinetics was derived from μ_1 and μ_2' of the elution peak profiles, respectively.[1,11$-$14] Some physical properties of the packing materials (such as the internal porosity) were derived from the pulse response data obtained using uracil and sodium nitrate as the inert tracers.

Data Analysis. In this study, the values of D_s were derived from μ_2' by subtracting the contributions to band broadening of several kinetic processes acting in the column, axial dispersion, external mass transfer, and pore diffusion. Only the basic information about the derivation procedure of the D_s data is briefly described in the following. Further details on the moment analysis method can be found in other references.[1,11$-$14]

First, the value of K was calculated from the first moment (μ_1) of the elution peak. The constant K is the ratio of the solute concentrations in the stationary and the mobile phase at equilibrium. The concentration in the stationary phase is defined as the weight of the sample compound per unit weight of the particulate packing materials. On the other hand, the expression of volumetric concentration is used for the mobile phase. The value of K (in units of cm^3/g) is derived from μ_1 by taking into account the hold-up time of the column, the weight of stationary phase in the column, and the void volume of the column. The intraparticle diffusivity (D_e) and the axial dispersion coefficient then were derived from μ_2' after subtracting the contribution of the external mass transfer to the band spreading. The contribution of intraparticle diffusion and that of the axial dispersion were separated by taking advantage of their different flow-rate dependence. The external mass-transfer coefficient (k_f) was estimated by the equation of Wilson$-$Geankoplis.[42] The Wilke$-$Chang equation was used to estimate the molecular diffusivity (D_m) of the sample compounds in the mobile-phase solvent.[1,43,44] It was also assumed that intraparticle diffusion consists of two parallel contributions: those due to pore diffusion and those due to surface diffusion.[13,14] The value of D_s was calculated by subtracting the contribution of pore diffusion to intraparticle diffusion. The pore diffusivity (D_p) was estimated from D_m, ϵ_p, the hindrance parameter (k_h), and the tortuosity factor (k_t) of the internal pores. The equation proposed by Satterfilder et al.[45] was used to estimate k_h from the ratio of the diameter of the sample molecule to the average pore diameter. The value of k_t was determined from the similar pulse response experiments, using uracil as the inert tracer. The contribution of the adsorption/desorption kinetics at the actual adsorption sites to μ_2' was assumed to be negligibly small in RPLC.[46]

Several corrections were also made accurately to derive D_s values from μ_2'. These corrections are described in the following.

1. Correction for Extra-Column Tubes. The retention time and the band dispersion experimentally measured were corrected for the contributions of the extra-column tubes between the injection valve and the column and between the column and the detector. These contributions were measured from the results of tracer experiments made without the column and were corrected to derive the values of K and D_s from μ_1 and μ_2', respectively.

2. Correction for Asymmetrical Peak Profiles. The influence of the peak distortion on the determination of μ_1 and μ_2' was corrected. The occurrence of asymmetrical (tailing or fronting) peaks has been explained based on several models.[1] In this study, the radial heterogeneity of the packing structure in the column was regarded as the only significant origin of the peak skewness.[47$-$49] More-accurate values of μ_1 and μ_2' were derived from the elution peak profiles by applying a correction procedure, using some basic information of the peak, i.e., the peak width at 10% and 50% peak height and the asymmetry factor at 10% height. Possible heterogeneous mass-transfer kinetics was not considered, because the surface of the alkyl ligands bonded silica gels seems to be energetically homogeneous. For instance, when C_{18}-silica gels are used as the stationary phase, (i) the phase equilibrium isotherm is usually accounted for by the simple Langmuir model[1,11,46,50] and (ii) both Q_{st} and E_s were almost constant, irrespective of the amount of sample compounds adsorbed.[11] These experimental observations imply the apparent uniformity of the surface of C_{18}-silica gels.

3. Correction for the Injection Volume of Sample Solution. The contributions of μ_1 and μ_2' of the sample pulses introduced at the inlet of the column were neglected, because of the extremely small size of the sample solution injected. As described previously, for instance, the injection volume of the sample solution of *n*-hexylbenzene was ca. 300 μL, because of the low solubility of the compound into the mobile-phase solvent. It is not small in comparison with the conventional sample injection volume in LC. However, the retention volume of *n*-hexylbenzene is $\sim$2 orders of magnitude or more larger than the sample injection volume. The retention of *n*-hexylbenzene is so strong that the volume of the sample injected provides substantially no influence on the moment analysis of the elution peaks.

4. Correction for the External Mass-Transfer Kinetics. As mentioned previously, the contribution of the external mass-transfer resistance to μ_2' was subtracted beforehand during the determination of D_e. An uncertainty in the estimation of k_f provides an influence on the results of the second moment analysis. In this study, k_f was estimated by the Wilson$-$Geankoplis equation.[42] For instance, a value, $k_f = 3.4 \times 10^{-2}$ cm/s, was obtained for benzene at 298 K when the superficial velocity of the mobile phase solvent is 0.12 cm/s. According to the equation proposed by Kataoka et al.,[51] a slightly different value, $k_f = 2.6 \times 10^{-2}$ cm/s, was obtained under the same

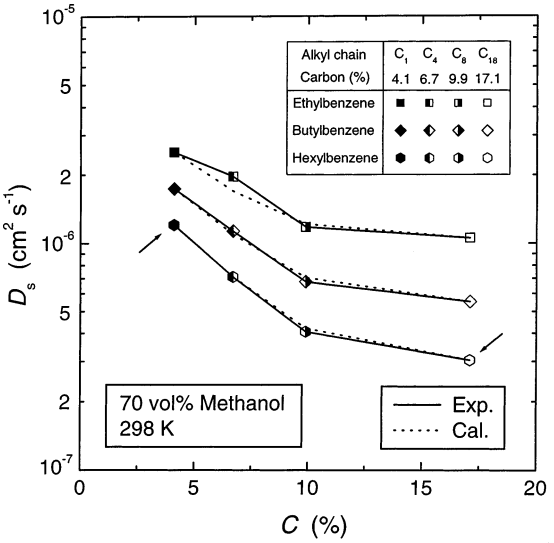

Figure 1. Plot of the surface diffusion coefficient (D_s) versus the carbon content of the stationary phases.

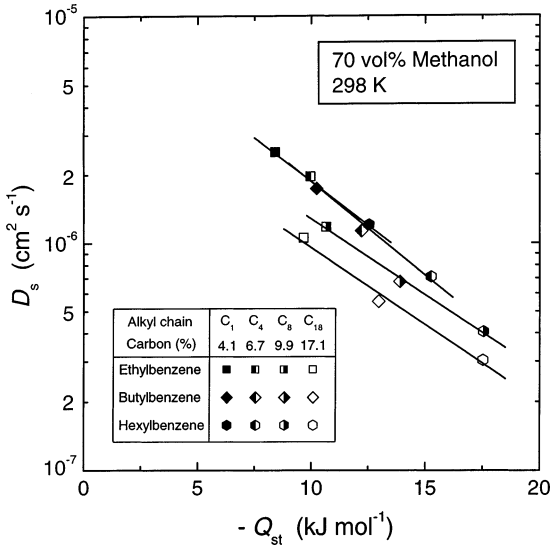

Figure 2. Plot of D_s versus the isosteric heat of adsorption ($-Q_{st}$).

conditions. The corresponding values of D_s were 7.2×10^{-6} cm^2/s and 5.8×10^{-6} cm^2/s, respectively. These two values differ by ca. 25%. The influence of variation in the estimated value of k_f on D_s values is not so large, because the contribution of the external mass-transfer resistance to μ_2' is usually ~20%−30% in some RPLC systems.[11]

(5) Correction for Pore Diffusion. The contribution of D_p to D_e is corrected when D_s is calculated from D_e. As mentioned previously, D_p was calculated from D_m, ϵ_p, k_h, and k_t. The accuracy in the estimation of D_m affects the accuracy in the estimation of D_s. In this study, D_m of the sample molecules in the mobile-phase solvent was calculated using the Wilke−Chang equation.[1,43,44] It is considered that this correlation provides estimates of D_m that are in error by less than ~10%.[43] Surface diffusion is usually the major contribution to intraparticle diffusion. For example, the contribution of surface diffusion to the overall mass transfer inside C_{18}-silica gel particles was large and as much as ~85%−95%.[11] Because of the predominant contribution of surface diffusion to intraparticle diffusion, the influence of small variation in D_p (and, hence, in D_m) on the estimate of D_s is small.

To derive a more-accurate value of D_s, we made the corrections described previously for some of the parameters affecting the original experimental data of μ_1 and μ_2' and for the parallel contributions of diffusive molecular migration processes other than surface diffusion. These corrections are responsible for the error made in the determination of D_s, which is estimated at ~5%−10%.[11,12] In addition, in this study, the pulse response experiments were conducted under such conditions that the influence of some sources on the peak broadening as described previously is minimized. Because relatively large particles of the alkyl ligands bonded silica gels were used as the packing materials, the original values of μ_2' attributed to the band broadening in the column were relatively large.

Results and Discussion

Dependence of D_s on the Retention. The solid lines in Figure 1 illustrate the correlation experimentally observed between D_s and the carbon content of the stationary phases. The value of D_s gradually decreases as the carbon content increases. However, the value of D_s also begins to plateau when the carbon content exceeds a critical value (~10%), a value that seems to be approximately the same for all the compounds studied. The results in Figure 1 imply that molecular migration by surface diffusion is restricted by the adsorptive interaction between the sample molecules and the stationary-phase surface.

Previously,[11,12,15−17,39,52−54] we studied surface diffusion phenomena from various points of view, including the retention equilibrium, its thermodynamics, and its extrathermodynamics. On the basis of these results, we proposed a "surface-restricted molecular diffusion model" as a first approximation to interpret the intrinsic characteristics and mechanisms of surface diffusion:

$$D_s \approx D_m \exp\left[\frac{-\alpha(-Q_{st})}{RT}\right] \quad (1)$$

where R is the gas constant and T is the absolute temperature. The solid lines in Figure 2 illustrate the linear correlation between ln D_s and Q_{st}. They are almost parallel. The slope of the linear lines corresponds to the ratio of the proportional coefficient (α) to RT. The value of ln D_s decreases almost linearly as $-Q_{st}$ increases, suggesting that surface diffusion is restricted by the retention strength.

Enthalpy−Entropy Compensation of Surface Diffusion. The temperature dependence of D_s was analyzed according to the Arrhenius equation:

$$D_s = D_{s0} \exp\left(\frac{-E_s}{RT}\right) \quad (2)$$

Figure 3 shows a plot between the frequency factor of surface diffusion (D_{s0}) and its activation energy (E_s), using the values measured for *n*-hexylbenzene on the different columns used. The linear correlation between ln D_{s0} and E_s suggests that there is an EEC for surface diffusion, regardless of the modification conditions of the alkyl-ligand-bonded silica gels. The slope of the straight line in Figure 3 indicates a compensation temperature (T_c) of ~4.2×10^2 K. Unfortunately, there are no other values of T_c for surface diffusion with which to compare our own.[18,19] We reported a T_c value of ca. 6.0×10^2 K for the surface diffusion of *p*-alkylphenol derivatives in the RPLC system consisting of a C_{18}-silica gel column and a mixture of methanol and water (70/30, v/v).[19] Similarly, a value of $T_c = 3.7 \times 10^2$ K was reported for the surface diffusion of benzene derivatives and naphthalene in the RPLC system using a C_{18}-silica gel column and an aqueous solution of tetrahydrofuran (50 vol %).[18]

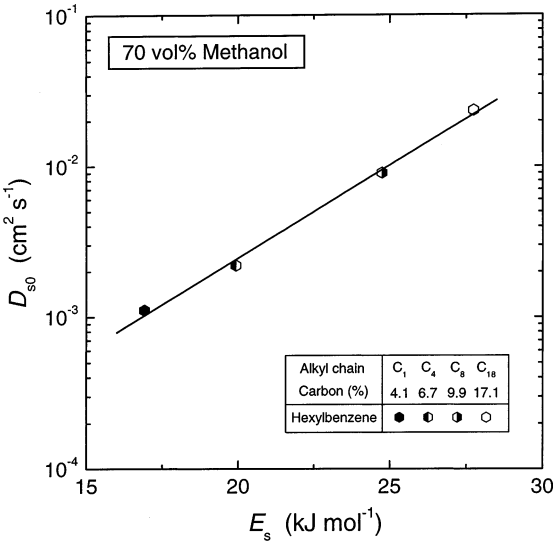

Figure 3. Plot of the frequency factor (D_{s0}) versus the activation energy of surface diffusion (E_s).

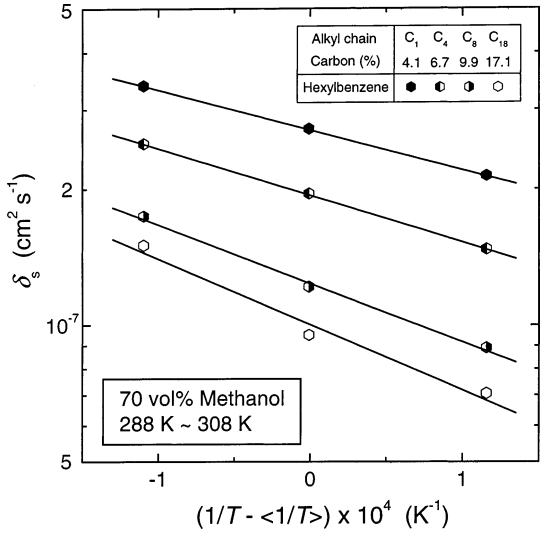

Figure 4. Plot of the normalized D_s coefficient (δ_s) versus $(1/T - \langle 1/T \rangle)$.

The value of T_c determined for surface diffusion in this study is on the same order of magnitude as the previous results.

In this study, we try to clarify, from the viewpoints of thermodynamics and extrathermodynamics, some of the characteristics of surface diffusion in RPLC systems, using silica gels bonded with alkyl ligands of different chain lengths. The carbon content (see Figure 1, abscissa) is a primary parameter that represents approximately the amount of alkyl ligands on the surface of the base silica gel. It is dependent on both the density and length of alkyl ligands. In addition, the ligand density also is dependent on the length of the main alkyl chains, even if we use the same base silica gel to prepare the stationary phases. Surface diffusion data on silica gels bonded with different alkyl ligands should not be compared directly. The data should be analyzed based on the surface diffusion normalized by the ligand density. No hydrophobic adsorption occurs when there are no alkyl ligands bonded to the surface of the base silica gel. Under such conditions, no surface diffusion occurs either. As a first approximation, we assumed that D_s is proportional to the ligand density (σ). It is expected that the higher the ligand density, the higher the surface diffusion mass flux per unit area and per unit time, for the same concentration gradient. We introduce a hypothetical value of the surface diffusion coefficient (δ_s), which would be measured using silica gel particles chemically modified with an alkyl ligand of unit density. The value of δ_s is calculated as the ratio of D_s to σ. We analyze experimental data of δ_s, rather than D_s.

The temperature dependence of δ_s is then analyzed using an equation similar to eq 2:

$$\ln \delta_s = -\frac{\Delta H^{=}}{RT} + \frac{\Delta S^{=}}{R} + \ln\left(\frac{\lambda^2 k_B T}{h}\right) \qquad (3)$$

where $\Delta H^{=}$ and $\Delta S^{=}$ are the enthalpy and the entropy of surface diffusion, respectively. The superscript "=" refers to thermodynamic parameters measured by analyzing the temperature dependence of δ_s. The parameters k_B and h are the Boltzmann and Planck constants, respectively. According to the absolute rate theory,[55] an estimate of the distance between two equilibrium positions ($\lambda = 3 \times 10^{-8}$ cm) was derived from the D_s of various molecules, which are on the order of 10^{-6} cm^2/s in methanol/water (70/30, v/v) at 298 K.[11,17] The analysis of the temperature dependence of the rate coefficient based on Arrhenius equation is one of the usual methods of estimating ΔH and ΔS associated with a kinetic process. However, Krug and co-workers[25−27] warned that a linear correlation can be observed between ΔH and ΔS, even when there is no real EEC effect. This apparent EEC is caused by errors made in the determination of the two thermodynamic parameters, based on the linear regressions of the Arrhenius plots. They showed that, in the case of an apparent EEC, the slope and the correlation coefficient of the linear correlation between ΔH and ΔS are equal to the harmonic mean temperature (T_{hm}) and are close to unity, respectively. They also proposed four different methods to clarify whether the linear correlation between ΔH and ΔS results from substantial physicochemical effects or from the statistical compensation due to the experimental errors.[25−27] We need to check our experimental data by applying the four methods proposed by Krug and co-workers to demonstrate that the EEC relationship proposed is real. In the following, the experimental data of surface diffusion obtained in this study were analyzed on the basis of the four approaches of Krug and co-workers.[25−27]

1. Plot of $\Delta H^{=}$ vs $\Delta G^{=}_{T_{hm}}$. If there is a real EEC for surface diffusion, the plot of $\Delta H^{=}$ vs $\Delta G^{=}_{T_{hm}}$ ($\Delta G^{=}$ at T_{hm}) should be linear. Krug and co-workers recommended that ln δ_s should be plotted against $(1/T - \langle 1/T \rangle)$, rather than the reciprocal of T, to derive the thermodynamic parameters more accurately. The bracketed terms ($\langle ... \rangle$) indicate an average value. Figure 4 shows linear correlations between ln δ_s and $(1/T - \langle 1/T \rangle)$. The values of $\Delta H^{=}$ and $\Delta G^{=}_{T_{hm}}$ for surface diffusion were respectively calculated from the slope and the intercept of the linear regressions in Figure 4:[25−27]

$$\Delta H = -R(\text{slope}) - RT_{hm} \qquad (4)$$

$$\Delta G^{=}_{T_{hm}} = -RT_{hm}(\text{intercept}) + RT_{hm} \ln\left(\frac{\lambda^2 e k_B T}{h}\right) - RT_{hm} \qquad (5)$$

where e is the base of the natural logarithm. A linear correlation is observed between $\Delta H^{=}$ and $\Delta G^{=}_{T_{hm}}$ in Figure 5. The compensation temperature obtained for surface diffusion ($T_c^{=}$) is 3.9×10^2 K for *n*-hexylbenzene, as derived from the slope of the straight line in Figure 5, according to the relation $T_c = T_{hm}/\{1 - [1/(\text{slope})]\}$. This is slightly different from the previous value of T_c estimated from the slope of the linear line in Figure

TABLE 2: Calculation Results of the Compensation Temperatures Concerning Surface Diffusion

	$T_c^=$ (K)		Range of $T_c^=$ Values (K)[b]		
	calculated from Figure 5[a]	calculated using eq 7	minimum	maximum	confidence level, $(1-\alpha_s)\times 100$ (%)
ethylbenzene	3.9×10^2	3.7×10^2	3.1×10^2	4.2×10^2	80
n-butylbenzene	3.8×10^2	3.8×10^2	3.0×10^2	4.6×10^2	97.5
n-hexylbenzene	3.9×10^2	3.9×10^2	3.2×10^2	4.8×10^2	99

[a] Calculated from the slope of the linear correlation between $\Delta H^=$ and $\Delta G^=_{Thm}$ in Figure 5. [b] Range of $T_c^=$ calculated by eqs 6−8 at $(1-\alpha_s)\times 100\%$ confidence level.

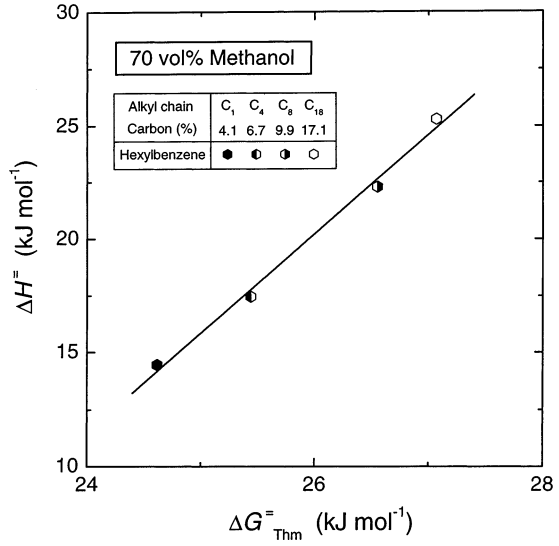

Figure 5. Plot of the enthalpy change of surface diffusion ($\Delta H^=$) versus the free-energy change at T_{hm} of surface diffusion ($\Delta G^=_{T_{hm}}$).

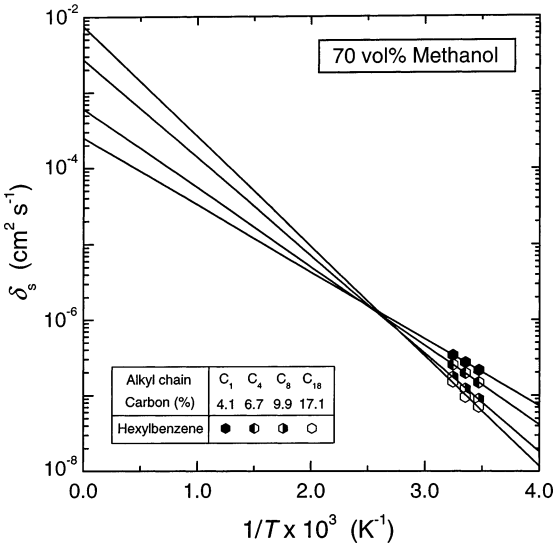

Figure 6. Temperature dependence of δ_s.

3 (4.2×10^2 K). This difference should probably be ascribed to the normalization of D_s values by σ.

2. Comparison of $T_c^=$ with T_{hm} (Hypothesis Test). The values of $T_c^=$ and T_{hm} should be compared with each other by applying the t-test (hypothesis test). The best estimate of $T_c^=$ should be sufficiently different from T_{hm} when a real EEC happens. Krug et al.[25] proposed the following equation to test the null hypothesis of $T_c^= = T_{hm}$. A minimum and maximum value of $T_c^=$ at an approximate $(1-\alpha_s)\times 100\%$ confidence level were calculated by the following equations:

$$T_c^=(\text{minimum}) = T_c^= - t_{m-2,1-\alpha_s}[V(T_c^=)]^{1/2} \qquad (6a)$$

$$T_c^=(\text{maximum}) = T_c^= + t_{m-2,1-\alpha_s}[V(T_c^=)]^{1/2} \qquad (6b)$$

with

$$T_c^= = \frac{\sum(\Delta H^= - \langle\Delta H^=\rangle)(\Delta S^= - \langle\Delta S^=\rangle)}{\sum(\Delta S^= - \langle\Delta S^=\rangle)^2} \qquad (7)$$

$$V(T_c^=) = \frac{\sum(\Delta H^= - \Delta G^=_{T_c^=} - T_c^=\Delta S^=)^2}{(m-2)\sum(\Delta S^= - \langle\Delta S^=\rangle)^2} \qquad (8)$$

where m is the number of ($\Delta H^=$ and $\Delta S^=$) data pairs and t is the value of the Student t for $(m-2)$ data points and a confidence level of $(1-\alpha_s)\times 100\%$.

The calculation results are reported in Table 2. The value of $T_c^=$ (3.9×10^2 K) calculated for *n*-hexylbenzene by eq 7 agrees fairly well with that of $T_c^=$ estimated from the slope of the linear correlation between $\Delta H^=$ and $\Delta G^=_{T_{hm}}$ in Figure 5. Similar values of $T_c^=$ were observed for the other two sample compounds. The $T_c^=$ values seem to be sufficiently different from T_{hm} (= 298 K). Table 2 lists the values of $T_c^=$ (minimum) and $T_c^=$ (maximum), which are calculated by eqs 6a and 6b. According to the t-test, the hypothesis of a coincidence of the slope of the $\Delta H^=$ vs $\Delta S^=$ plot ($T_c^=$) with T_{hm} can be rejected for surface diffusion, although the confidence level is different for the sample compounds.

3. Convergence of the Arrhenius Plots at $T_c^=$. Figure 6 shows the Arrhenius plots of *n*-hexylbenzene. The linear regression lines properly intersect in a small region of the plane. The compensation temperature estimated from the intersection point in Figure 6 is fairly close to the value of $T_c^=$ obtained as previously described.

4. Probability for the Intersection of the Arrhenius Plots. According to the *F*-test, the probability for the intersection was compared with that for a nonintersection, on the basis of the statistical data derived by an analysis of variance (ANOVA) procedure.[27] The probability for nonintersection was also compared to the precision of the experimental data in the same manner.

Table 3 lists the values of the mean sum of squares calculated. The mean sum of squares of the intersection (MS_{con}) is one or two orders of magnitude larger than that of the nonintersection (MS_{noncon}). The ratio MS_{con}/MS_{noncon} for *n*-butylbenzene and *n*-hexylbenzene is sufficiently larger than the *F*-value, $F(1, 2, 1-\alpha_s = 0.95) = 18.5$, although the ratio for ethylbenzene is slightly smaller than the *F*-value. It is indicated for *n*-butyl- and *n*-hexylbenzene that the probability for the intersection is high compared with that for nonintersection. On the other hand,

TABLE 3: Analysis of Variance (ANOVA) Table for Surface Diffusion of the Different Sample Compounds[a]

				Ethylbenzene ($p = 4$, $q = 3$)			*n*-Butylbenzene ($p = 4$, $q = 3$)			*n*-Hexylbenzene ($p = 4$, $q = 3$)		
	DF[b]	SS[c]	MS[d]	DF[b]	SS[c]	MS[d]	DF[b]	SS[c]	MS[d]	DF[b]	SS[c]	MS[d]
total	$pq - 1$	SS_T	MS_T	11	1.4	1.3×10^{-1}	11	1.9	1.7×10^{-1}	11	2.5	2.3×10^{-1}
rows (samples)	$p - 1$	SS_R	MS_R	3	8.0×10^{-1}	2.7×10^{-1}	3	1.3	4.3×10^{-1}	3	1.8	6.0×10^{-1}
columns (temperatures)	$q - 1$	SS_C	MS_C	2	5.5×10^{-1}	2.8×10^{-1}	2	6.1×10^{-1}	3.0×10^{-1}	2	7.4×10^{-1}	3.7×10^{-1}
interactions	$(p - 1)(q - 1)$	SS_{RC}	MS_{RC}	6	2.7×10^{-2}	4.5×10^{-3}	6	2.5×10^{-2}	4.1×10^{-3}	6	1.3×10^{-2}	2.2×10^{-3}
slope	$p - 1$	SS_S	MS_S	3	1.3×10^{-2}	4.2×10^{-3}	3	2.0×10^{-2}	6.7×10^{-3}	3	2.7×10^{-2}	8.9×10^{-3}
concurrence	1	SS_{con}	MS_{con}	1	1.1×10^{-2}	1.1×10^{-2}	1	1.9×10^{-2}	1.9×10^{-2}	1	2.7×10^{-2}	2.7×10^{-2}
nonconcurrence	$p - 2$	SS_{noncon}	MS_{noncon}	2	1.9×10^{-3}	9.6×10^{-4}	2	5.4×10^{-4}	2.7×10^{-4}	2	2.1×10^{-4}	1.0×10^{-4}
residuals	$(p - 1)(q - 2)$	SS_ϵ	MS_ϵ	3	1.4×10^{-2}	4.8×10^{-3}	3	4.8×10^{-3}	1.5×10^{-3}	3	-1.3×10^{-2}	-4.5×10^{-3}

[a] In this table, p is the number of the stationary phases and q is the number of experimental temperatures. [b] Degrees of freedom. [c] Sum of squares. [d] Mean sum of squares for each source of variation; MS = SS/DF.

the value of MS_{noncon} is smaller than the mean sum of squares of the residuals (MS_ϵ). In addition, the ratio of MS_{noncon} to MS_ϵ was sufficiently smaller than the corresponding F-value, $F(2, 3, 1 - \alpha_s = 0.95) = 9.55$. Although the negative value of MS_ϵ for *n*-hexylbenzene is probably unreasonable, it seems to result from calculation errors and suggest that the variation due to the measurement errors is quite small. It is concluded that the variation due to nonconcurrence is not greater than that due to the measurement errors at the $100\alpha_s$% level of significance.

Based on the results previously described, it is concluded that a real EEC for surface diffusion originates from substantial physicochemical effects that occur in the RPLC systems. The mechanism of surface diffusion in the RPLC systems seems to be similar, irrespective of the length of the alkyl chains bonded to the base silica gel.

Linear Free Energy Relationships for Surface Diffusion. A linear free energy relationship (LFER) is another extrathermodynamic relationship. The value of the free-energy variation, ΔG, associated with a chemical equilibrium is linearly correlated with that of a related kinetic process. LFERs can also be observed between different reaction equilibria or kinetic processes. The empirical correlations of thermodynamic quantities found in EEC and LFER have been used to demonstrate the mechanistic similarity of equilibrium or kinetic processes. In addition, the ΔG values of equilibrium and kinetic processes are assumed to consist of the sums of incremental contributions that are due to structural elements of molecules. The characteristics of reaction processes have also been studied from the viewpoints of molecular structural contributions by analyzing these two extrathermodynamic correlations.

1. Influence of the Change in RPLC Conditions on Surface Diffusion. Figure 7 shows the temperature dependence of δ_s of *n*-hexylbenzene. The values of δ_s (plots) at 288 and 308 K are compared with those at 298 K. Only the column temperature was changed. These plots seem to suggest an LFER between the δ_s values at the two temperatures. The slope of the linear correlation at 288 K seems to be slightly larger than that at 308 K.

In Figure 8, the value of δ_s of *n*-butylbenzene at the three temperatures are plotted against that of *n*-hexylbenzene at 298 K. In this case, both the nature of the compound and the temperature were simultaneously changed. Again, linear correlations seem to occur between the logarithms of δ_s for the two compounds at the three different temperatures.

2. A Model for Explaining the Change in Surface Diffusion. As shown in Figures 7 and 8, the mechanism of surface diffusion in RPLC is dependent on some experimental conditions. In the following, we try to develop a model based on EEC and LFER, which would provide an effective, comprehensive explanation of the variations of D_s.

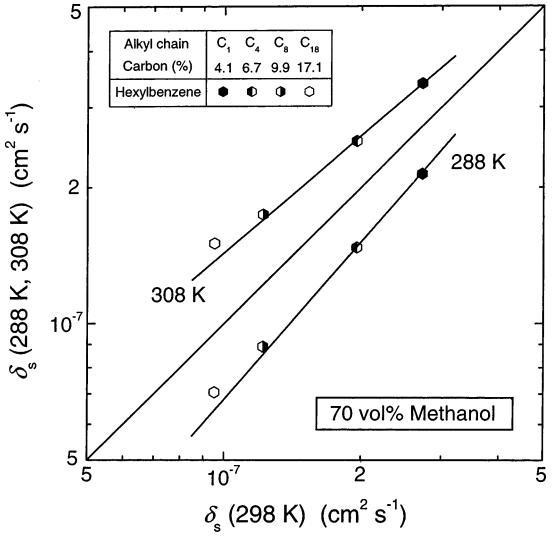

Figure 7. Correlation between δ_s values of *n*-hexylbenzene under different temperature conditions.

The free-energy change of surface diffusion ($\Delta G^{=}$) is related to δ_s as follows:

$$-\frac{\Delta G^{=\mathrm{REF}}_{T_1}}{RT_1} = \ln K^{=\mathrm{REF}}_{T_1} = \ln \delta^{\mathrm{REF}}_{sT_1} + \ln\left(\frac{h}{\lambda^2 k_B T_1}\right) \quad (9)$$

$$-\frac{\Delta G^{=\mathrm{SMP}}_{T_2}}{RT_2} = \ln K^{=\mathrm{SMP}}_{T_2} = \ln \delta^{\mathrm{SMP}}_{sT_2} + \ln\left(\frac{h}{\lambda^2 k_B T_2}\right) \quad (10)$$

where T_1 and T_2 denote the column temperatures and the superscripts "REF" and "SMP" denote the reference and the sample system, respectively. $K^{=}$ is the hypothetical equilibrium constant between a steady state and the transition state.[55] Note that $\lambda = 1$ when eqs 9 and 10 are written for first-order rate constants instead of δ_s.[55] As described in Figures 7 and 8, the values of $\Delta G^{=\mathrm{SMP}}_{T_2}$ are linearly correlated with those of $\Delta G^{=\mathrm{REF}}_{T_1}$. This confirms an LFER between the corresponding RPLC systems.

$$\ln \delta^{\mathrm{SMP}}_{sT_2} = A \ln \delta^{\mathrm{REF}}_{sT_1} + B \quad (11)$$

Substituting eqs 9 and 10 into eq 11 gives

$$\Delta G^{=\mathrm{SMP}}_{T_2} = A\left(\frac{T_2}{T_1}\right)\Delta G^{=\mathrm{REF}}_{T_1} + RT_2(A-1)\ln\left(\frac{h}{\lambda^2 k_B}\right) + RT_2(\ln T_2 - A \ln T_1) - RT_2 B \quad (12)$$

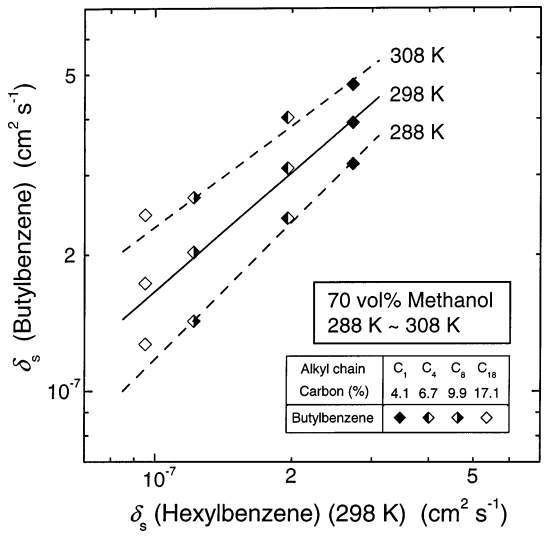

Figure 8. Correlation between δ_s values of *n*-butylbenzene and *n*-hexylbenzene under different temperature conditions.

Equation 12 formulates the LFER between the different RPLC conditions considered.

On the other hand, $\Delta G^{=}$ is the sum of an enthalpy change ($\Delta H^{=}$) and an entropy change ($\Delta S^{=}$), according to the Gibbs−Helmholtz relation.

$$\Delta G^{=} = \Delta H^{=} - T\Delta S^{=} \tag{13}$$

The following equation has been proposed to correlate $\Delta G^{=}$ of a molecule involved in hydrophobic interactions with a parameter describing a molecular property (X_m):[29,56]

$$\Delta G^{=} = a_g X_m + b_g \tag{14}$$

where a_g and b_g are the molecular thermodynamic parameters. The value of a_g is $\Delta G^{=}$ per unit value of the molecular property X_m and that of b_g is $\Delta G^{=}$ at $X_m = 0$. Various molecular properties can be taken for X_m (for instance, the surface area of the nonpolar part of the molecule or recurring structural elements, e.g., the number of methylene units in an alkyl chain). In this study, the number of C atoms in the alkyl ligands bonded to the base silica gel was changed. The number of methylene groups (C_n) in the alkyl ligands was used as X_m. The value of C_n includes the contribution of both the main alkyl chain and two methyl groups, because the packing materials used in this study were probably synthesized using alkyldimethylsilyl ligands.

Figure 9a shows the plots of $\Delta G^{=}$ at T_{hm} (298 K) versus C_n. Linear correlations are observed for the three plots corresponding to ethyl-, *n*-butyl-, and *n*-hexyl-benzene, for the C_1-, C_4-, and C_8-silica gels, respectively, although the plots of ethylbenzene show some scatter. The straight lines in Figure 9a demonstrate the validity of eq 14. On the other hand, the plots for the C_{18}-silica gel deviate considerably from the corresponding linear correlations. The value of $\Delta G^{=}$ tends toward a constant limit with increasing chain length. Similar observations were reported for the effect of the alkyl chain length on the retention and the separation factors, i.e., a linear correlation at short chain lengths and a limit at long lengths.[3,4,7,8] The carbon number corresponding to the critical chain length was reported to be between 6 and 14, irrespective of the mobile phase composition.[4] It was also reported that this critical length is dependent on the molecular size of the sample compound: the larger the sample molecule, the longer the critical length.[3,8] This probably results

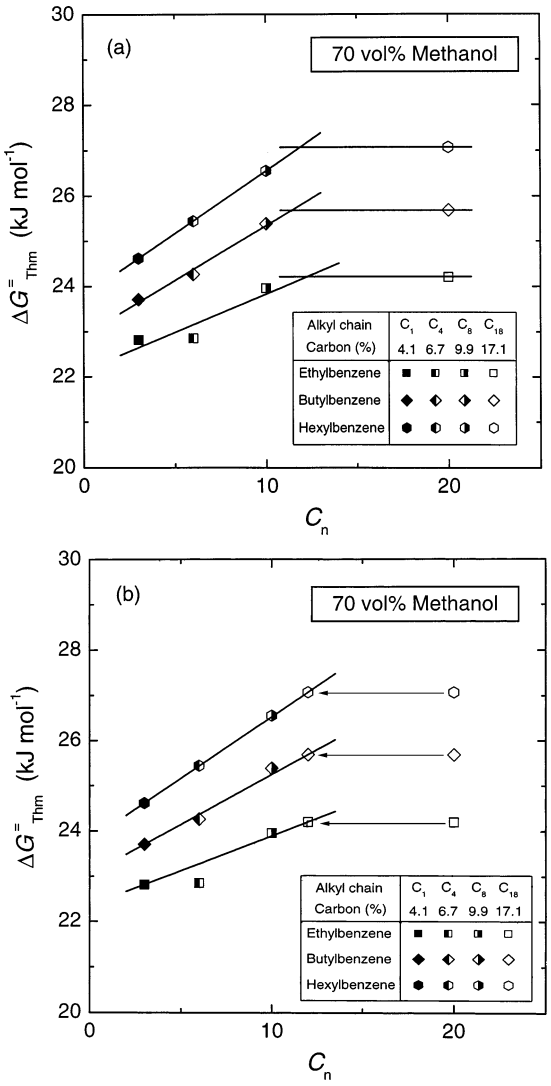

Figure 9. Plot of $\Delta G^{=}_{T_{hm}}$ versus the number of methylene groups (C_n). The values of $\Delta G^{=}_{T_{hm}}$ for C_{18}-silica gel are plotted at (a) $C_n = 20$ and (b) $C_n = 12$.

from an effect of the conformation of long alkyl chains. The position of the intersection of the two lines for each compound in Figure 9a implies that the contribution of the C_{18} chain to the hydrophobic interactions with the sample molecules are similar to that of the C_{10} alkyl chain. In Figure 9b, the value for the C_{18}-silica gel is shifted to $C_n \approx 12$.

Similar representations may be written for the variations of the enthalpy and the entropy, using the corresponding molecular thermodynamic parameters (a_h, b_h, a_s, and b_s).[29,56]

$$\Delta H^{=} = a_h X_m + b_h \tag{15}$$

$$\Delta S^{=} = a_s X_m + b_s \tag{16}$$

Figure 10a shows the values of $\Delta H^{=}$ as a function of C_n. Although the plots for ethylbenzene are again scattered to some extent, linear correlations are observed between $\Delta H^{=}$ and C_n, suggesting the correctness of eq 15. Figure 10b similarly shows the correlation of $\Delta S^{=}$ with C_n. Although Figure 10b shows a larger degree of scattering than Figures 9b and 10a, it is probable that $\Delta S^{=}$ is also linearly correlated with C_n, because both $\Delta G^{=}$ and $\Delta H^{=}$ are certainly taken into consideration by linear functions of C_n. Similar to Figure 9b, the values of the two thermodynamic parameters ($\Delta H^{=}$ and $\Delta S^{=}$) for the C_{18}-silica

TABLE 4: Molecular Thermodynamic Parameters

	$\Delta H^{=}$ vs C_n		$\Delta S^{=}$ vs C_n		
	a_h (kJ/mol)	b_h (kJ/mol)	a_s (kJ mol^{-1} K^{-1})	b_s (kJ mol^{-1} K^{-1})	$T_c^{=}$ (K)[a]
ethylbenzene	0.83	1.0×10^1	2.2×10^{-3}	-3.9×10^{-2}	3.8×10^2
n-butylbenzene	1.0	9.7	2.7×10^{-3}	-4.5×10^{-2}	3.9×10^2
n-hexylbenzene	1.2	1.1×10^1	3.1×10^{-3}	-4.4×10^{-2}	3.9×10^2

[a] $T_c^{=} = a_h/a_s$.

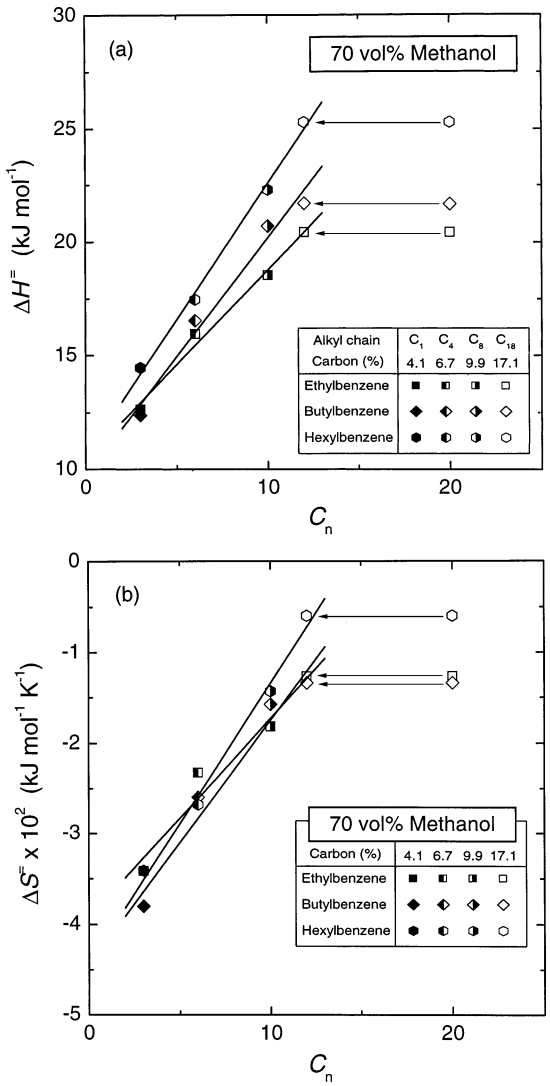

Figure 10. Plot of (a) $\Delta H^{=}$ vs C_n and (b) $\Delta S^{=}$ vs C_n. The values of the two thermodynamic parameters for C_{18}-silica gel are plotted at $C_n = 12$.

gel were plotted at $C_n = 12$ in Figures 10a and 10b. Table 4 lists the resulting values of the slope (a) and intercept (b). Using the slopes of the straight lines between $\Delta H^{=}$ and C_n (a_h) and between $\Delta S^{=}$ and C_n (a_s), $T_c^{=}$ can be written as[29]

$$T_c^{=} = \frac{a_h}{a_s} \tag{17}$$

Table 4 also lists the ratios of a_h to a_s, which are in fairly good agreement with the values of $T_c^{=}$ in Table 2.

Differentiation of both sides of eq 12 with respect of C_n gives

$$\frac{\partial \Delta G_{T_2}^{=\mathrm{SMP}}}{\partial C_n} = A\left(\frac{T_2}{T_1}\right)\frac{\partial \Delta G_{T_1}^{=\mathrm{REF}}}{\partial C_n} \tag{18}$$

The following equation is derived from a combination of eqs 13, 15, and 16.

$$\Delta G^{=} = \Delta H^{=} - T\Delta S^{=} = (a_h C_n + b_h) - T(a_s C_n + b_s) \tag{19}$$

Substituting eq 19 into eq 18 and rearranging gives

$$A = \frac{a_s^{\mathrm{SMP}} T_1 (T_c^{=\mathrm{SMP}} - T_2)}{a_s^{\mathrm{REF}} T_2 (T_c^{=\mathrm{REF}} - T_1)} \tag{20}$$

where a_s^{REF} and a_s^{SMP} are the increments of $\Delta S^{=}$ corresponding to the addition of one methylene unit in the alkyl ligands, in the reference and the sample systems, respectively. Equation 20 shows that A is dependent on the temperature and that this temperature dependence is correlated with T_1, T_2, $T_c^{=\mathrm{REF}}$, and $T_c^{=\mathrm{SMP}}$.

On the other hand, substituting eq 19 into eq 12 gives B (eq 11), as follows:

$$B = \frac{1}{RT_2}\left[A\left(\frac{T_2}{T_1}\right)(b_h^{\mathrm{REF}} - T_1 b_s^{\mathrm{REF}}) - (b_h^{\mathrm{SMP}} - T_2 b_s^{\mathrm{SMP}})\right] + (A-1)\ln\left(\frac{h}{\lambda^2 k_B}\right) + (\ln T_2 - A \ln T_1) \tag{21}$$

Equations 20 and 21 show the dependence of the slope and the intercept of the LFER in eq 12 on the molecular thermodynamic parameters (a and b) in eqs 15 and 16, the compensation temperatures ($T_c^{=}$), and experimental temperature (T).

3. Interpretation of the Variations of D_s on the Basis of the EEC. Equations 20 and 21 should explain the correlation between the properties of surface diffusion of two chromatographic systems effectively. When only the temperature is changed, eqs 20 and 21 should be modified as follows.

$$A = \frac{T_1 (T_c^{=} - T_2)}{T_2 (T_c^{=} - T_1)} \tag{22}$$

$$B = \frac{1}{RT_2}\left[A\left(\frac{T_2}{T_1}\right)(b_h - T_1 b_s) - (b_h - T_2 b_s)\right] + (A-1)\ln\left(\frac{h}{\lambda^2 k_B}\right) + (\ln T_2 - A \ln T_1) \tag{23}$$

The solid lines in Figure 7 were calculated using eqs 22 and 23 and taking $T_1 = 298$ K and $T_2 = 288$ or 308 K for the δ_s values of *n*-hexylbenzene. Although the actual symbols for the C_{18}-silica gel deviate slightly from the solid lines, the other three experimental data points lay on the corresponding straight lines, demonstrating the validity of the model developed for explaining the temperature dependence of δ_s (hence of D_s).

When the temperature is constant, eqs 20 and 21 become

$$A = \frac{a_s^{SMP}(T_c^{=SMP} - T)}{a_s^{REF}(T_c^{=REF} - T)} \quad (24)$$

$$B = \frac{1}{RT}[A(b_h^{REF} - Tb_s^{REF}) - (b_h^{SMP} - Tb_s^{SMP})] + (A-1)\ln\left(\frac{h}{\lambda^2 k_B T}\right) \quad (25)$$

The solid line in Figure 8 was calculated using eqs 24 and 25 at constant temperature (298 K). The two dashed lines in Figure 8 were similarly calculated using eqs 20 and 21, because, in that case, both the nature of the compounds and the temperature were simultaneously changed. Again, all the experimental data overlay the corresponding straight lines. This shows that eqs 20 and 21 are useful to analyze the variations of δ_s and D_s with some of the RPLC experimental conditions.

4. Estimation of the Value of D_s. The results described previously show that it should be possible to estimate the value of δ_s—and, hence, D_s—under various RPLC experimental conditions from a limited number of experimental values of D_s. In the following, three RPLC conditions (the nature of the compounds, the length of the bonded alkyl chains, and the temperature) were simultaneously changed. We calculated D_s for three compounds (ethyl-, *n*-butyl-, and *n*-hexyl-benzene) between 288 and 308 K, on RPLC packing materials bonded to C_1-, C_4-, C_8-, and C_{18}-alkyl chains, in a methanol/water (70/30, v/v) solution, using only the two experimental values for *n*-hexylbenzene, at 298 K, on C_1- and C_{18}-silica gels. First, the values of D_s for the three compounds were derived at a given temperature on the C_1- and C_{18}-silica gels from those of *n*-hexylbenzene, using eqs 20 and 21 and the molecular thermodynamic parameters (*a* and *b*) listed in Table 4 and the compensation temperatures ($T_c^{=}$) listed in Tables 2 and 4. The values of D_s on the C_4- and C_8-silica gels then were derived using the linear correlations between $\Delta G^{=}$ and C_n for each compound, as illustrated in Figure 9b. Linear functions of $\Delta G^{=}$ with C_n were derived from the two values of δ_s for the C_1- and C_{18}-silica gels estimated beforehand.

The dotted lines in Figure 1 compare the values of D_s at 298 K thus calculated with those experimentally measured. The arrows in Figure 1 indicate the original two data points experimentally measured, from which the values of D_s were estimated under different experimental conditions. The solid and the dotted lines connect the experimental and the estimated values of D_s, respectively. These two lines are very similar, almost identical. The plots of D_s for the C_4- and C_8-silica gels are almost overlaid. These results confirm the validity of the assumption made, that the contributions of the C_{18} alkyl chain to the hydrophobic interactions with the sample molecules are almost the same as those of a C_{10} alkyl chain. The increment of $\Delta G^{=}$ due to one methylene group is the same for C_n between C_1 and C_8. Similarly, in Figure 11, the values of D_s estimated at 288−308 K are compared with the corresponding experimental data. Again, the two arrows in Figure 11 indicate the values measured for *n*-hexylbenzene at 298 K on the C_1- and the C_{18}-silica gels. The symbols in Figure 11 are slightly scattered around a solid line having a slope of unity. These results prove the validity of our model of surface diffusion based on the EEC. This model (eqs 20 and 21) provides for a comprehensive explanation of the intrinsic characteristics of surface diffusion in RPLC systems, from the thermodynamic and the extrathermodynamic points of view.

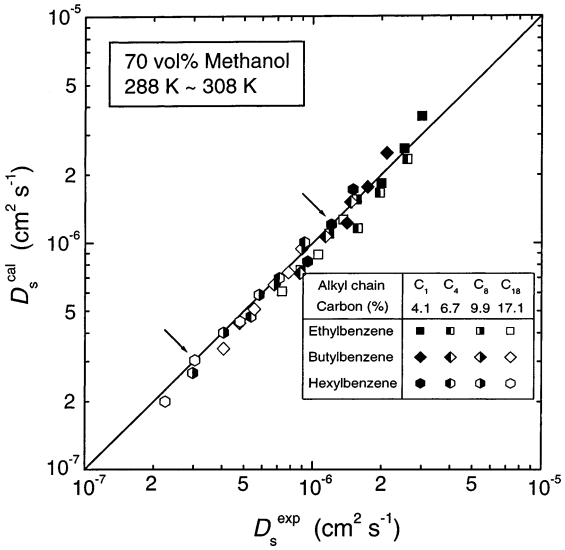

Figure 11. Comparison of D_s values estimated with those measured experimentally.

Conclusion

Our results demonstrate that there is an actual enthalpy−entropy compensation (EEC) relationship for surface diffusion in reversed-phase liquid chromatography (RPLC) on silica gels bonded to *n*-alkyl ligands that have 1−18 carbon atoms, where the four criteria developed by Krug et al. being satisfied. The compensation temperature is ∼390 K. These results allowed the development of a simple model based on this EEC that explains the LFER observed between the surface diffusion coefficients measured under different RPLC conditions. This model permits a reasonably accurate estimation of the surface diffusion coefficient under a wide range of experimental conditions from only a few experimental measurements. The error that is made is approximately ±20%, regardless of the nature of the compounds, the length of the bonded alkyl chain of the RPLC packing material, and the temperature.

Recently, various types of new packing materials, e.g., monolithic phases, have been proposed to achieve fast separations with high-efficiency columns. Their performance relies heavily on the intrinsic structural characteristics of the mesopores and macropores of these stationary phases. It is essential to acquire the detailed information required to understand the kinetic processes in these new types of stationary phases. As was noted 40 years ago,[57] the contribution of surface diffusion to mass-transfer mechanisms in the particles of chromatographic column is of major importance. The results and conclusions of this work should be helpful to clarify the characteristics and mechanisms of mass-transfer kinetics in the stationary phases used in chromatography and to promote the development of novel separation media.

Symbols

a	slope of the linear correlation between a thermodynamic property and X_m
A	slope of LFER
b	intercept of the linear correlation between a thermodynamic property and X_m
B	intercept of LFER
C_n	number of methylene groups
D_e	intraparticle diffusivity (m^2/s)
D_m	molecular diffusivity (m^2/s)
D_p	pore diffusivity (m^2/s)

D_s	surface diffusion coefficient (m^2/s)
D_{s0}	frequency factor of surface diffusion (m^2/s)
ΔG	free-energy change (J/mol)
E_s	activation energy of surface diffusion (J/mol)
h	Planck's constant (J s)
ΔH	enthalpy change (J/mol)
k_B	Boltzmann's constant (J/K)
k_f	external mass-transfer coefficient (m/s)
k_h	hindrance parameter
k_t	tortuosity factor
K	adsorption equilibrium constant (m^3/g)
m	number of (ΔH and ΔS) data pairs
MS	mean sum of squares
Q_{st}	isosteric heat of adsorption (J/mol)
R	gas constant (J mol^{-1} K^{-1})
ΔS	entropy change (J mol^{-1} K^{-1})
T	absolute temperature (K)
T_c	compensation temperature (K)
T_{hm}	harmonic mean of experimental temperatures (K)
X_m	property of molecule

Greek Symbols

α	proportional coefficient in eq 1
α_s	statistical level of significance
δ_s	D_s value normalized by σ (m^2/s)
ϵ_e	column void fraction (external porosity)
ϵ_p	porosity of the stationary phase particle (internal porosity)
λ	distance between two equilibrium positions (m)
μ_1	first absolute moment (s)
μ_2'	second central moment (s^2)
ρ_p	particle density (kg/m^3)
σ	alkyl ligand density (mol/m^2)

Superscripts

cal	calculated
exp	experimental
REF	reference
SMP	sample
=	thermodynamic parameters measured by analyzing temperature dependence of δ_s

Subscripts

con	concurrence
g	free-energy change
h	enthalpy change
noncon	nonconcurrence
s	entropy change
T_c	compensation temperature
T_{hm}	harmonic mean of experimental temperatures
T_1	temperature condition 1
T_2	temperature condition 2
ϵ	measurement errors
1	condition 1
2	condition 2

References and Notes

(1) Guiochon, G.; Golshan-Shirazi, S.; Katti, A. M. *Fundamentals of Preparative and Nonlinear Chromatography*; Academic Press: Boston, 1994.

(2) Sander, L. C.; Wise, S. A. *Crit. Rev. Anal. Chem.* **1987**, *18*, 299−415.

(3) Löchmuller, C. H.; Wilder, D. R. *J. Chromatogr. Sci*. **1979**, *17*, 574−579.

(4) Berendsen, G. E.; de Galan, L. *J. Chromatogr*. **1980**, *196*, 21−37.

(5) Tchapla, A.; Colin, H.; Guiochon, G. *Anal. Chem.* **1984**, *56*, 621−625.

(6) Tchapla, A.; Heron, S.; Colin, H.; Guiochon, G. *Anal. Chem.* **1988**, *60*, 1443−1448.

(7) Tchapla, A.; Heron, S.; Lesellier, E.; Colin, H. *J. Chromatogr. A* **1993**, *656*, 81−112.

(8) Lork, K. D.; Unger, K. K. *Chromatographia* **1988**, *26*, 115−119.

(9) Karch, K.; Sebastian, I.; Halasz, I. *J. Chromatogr*. **1976**, *122*, 3−16.

(10) Knox, J. H.; Pryde, A. *J. Chromatogr*. **1975**, *112*, 171−188.

(11) Miyabe, K.; Guiochon, G. *Adv. Chromatogr.* **2000**, *40*, 1−113.

(12) Miyabe, K.; Guiochon, G. *J. Sep. Sci.* **2003**, *26*, 155−173.

(13) Ruthven, D. M. *Principles of Adsorption & Adsorption Processes*; Wiley: New York, 1984.

(14) Suzuki, M. *Adsorption Engineering*; Kodansha/Elsevier: Tokyo, 1990.

(15) Miyabe, K.; Guiochon, G. *J. Phys. Chem. B* **1999**, *103*, 11086−11097.

(16) Miyabe, K.; Guiochon, G. *Anal. Chem.* **2000**, *72*, 1475−1489.

(17) Miyabe, K.; Guiochon, G. *Anal. Chem.* **2001**, *73*, 3096−3106.

(18) Miyabe, K.; Sotoura, S.; Guiochon, G. *J. Chromatogr. A* **2001**, *919*, 231−244.

(19) Miyabe, K.; Guiochon, G. *Anal. Chem.* **2002**, *74*, 5754−5765.

(20) Leffler, J. E.; Grunwald, E. *Rates and Equilibria of Organic Reactions*; Wiley: New York, 1963.

(21) Hammett, L. P. *Physical Organic Chemistry*; McGraw−Hill: New York, 1970.

(22) Exner, O. *Nature* **1964**, *201*, 488−490.

(23) Exner, O. *Prog. Phys. Org. Chem.* **1973**, *10*, 411−482.

(24) Exner, O. *Prog. Phys. Org. Chem.* **1990**, *18*, 129−161.

(25) Krug, R. R.; Hunter, W. G.; Grieger, R. A. *J. Phys. Chem*. **1976**, *80*, 2335−2341.

(26) Krug, R. R.; Hunter, W. G.; Grieger, R. A. *J. Phys. Chem*. **1976**, *80*, 2341−2351.

(27) Krug, R. R. *Ind. Eng. Chem. Fundam.* **1980**, *19*, 50−59.

(28) Boots, H. M. J.; de Bokx, P. K. *J. Phys. Chem*. **1989**, *93*, 8240−8243.

(29) Vailaya, A.; Horváth, C. *J. Phys. Chem*. **1996**, *100*, 2447−2455.

(30) Colin, H.; Diez-Masa, J. C.; Guiochon, G.; Czajkowska, T.; Miedziak, I. *J. Chromatogr.* **1978**, *167*, 41−65.

(31) Melander, W. R.; Campbell, D. E.; Horváth, C. *J. Chromatogr*. **1978**, *158*, 215−225.

(32) Melander, W. R.; Chen, B. K.; Horváth, C. *J. Chromatogr*. **1979**, *185*, 99−109.

(33) Miyabe, K.; Guiochon, G. *Anal. Chem.* **2002**, *74*, 5982−5992.

(34) Melander, W. R.; Campbell, D. E.; Horváth, C. *J. Chromatogr*. **1978**, *158*, 215−225.

(35) Riley, C. M.; Tomlinson, E.; Jefferies, T. M. *J. Chromatogr*. **1979**, *185*, 197−224.

(36) Riley, C. M.; Tomlinson, E.; Hafkenscheid, T. L. *J. Chromatogr*. **1981**, *218*, 427−442.

(37) de Bokx, P. K.; Boots, H. M. J. *J. Phys. Chem*. **1989**, *93*, 8243−8248.

(38) Miyabe, K.; Guiochon, G. *J. Chromatogr. A* **2000**, *903*, 1−12.

(39) Miyabe, K.; Guiochon, G. *Anal. Sci.* **2001**, *17* (Supplement), i209−i212.

(40) Karger, B. L.; Gant, J. R.; Hartkopf, A.; Weiner, P. H. J. *Chromatogr*. **1976**, *128*, 65−78.

(41) Wells, M. J. M.; Clark, C. R. *Anal. Chem*. **1981**, *53*, 1341−1345.

(42) Wilson, E. J.; Geankoplis, C. J. *Ind. Eng. Chem. Fundam*. **1966**, *5*, 9−14.

(43) Reid, R. C.; Prausnitz, J. M.; Sherwood, T. K. *The Properties of Gases and Liquids*; McGraw−Hill: New York, 1977.

(44) Bird, R. B.; Stewart, W. E.; Lightfoot, E. N. *Transport Phenomena*; Wiley: New York, 2002.

(45) Satterfield, C. N.; Colton, C. K.; Pitcher, Jr., W. H. *AIChE J*. **1973**, *19*, 628−635.

(46) Miyabe, K.; Guiochon, G. *Anal. Chem.* **2000**, *72*, 5162−5171.

(47) Miyabe, K.; Guiochon, G. *J. Chromatogr. A* **1999**, *830*, 263−274.

(48) Miyabe, K.; Guiochon, G. *J. Chromatogr. A* **1999**, *830*, 29−39.

(49) Miyabe, K.; Guiochon, G. *J. Chromatogr. A* **1999**, *857*, 69−87.

(50) Miyabe, K.; Guiochon, G. *J. Chromatogr. A* **2000**, *890*, 211−223.

(51) Kataoka, T.; Yoshida, H.; Ueyama, K. *J. Chem. Eng. Jpn.* **1972**, *5*, 132−136.

(52) Miyabe, K.; Guiochon, G. *Anal. Chem.* **1999**, *71*, 889−896.

(53) Miyabe, K.; Guiochon, G. *J. Phys. Chem. B* **2001**, *105*, 9202−9209.

(54) Miyabe, K.; Guiochon, G. *J. Chromatogr. A* **2002**, *961*, 23−33.

(55) Glasstone, S.; Laidler, K. J.; Eyring, H. *The Theory of Rate Processes*; McGraw−Hill: New York, 1964.

(56) Lee, B. *Proc. Natl. Acad. Sci. U.S.A.* **1991**, *88*, 5154−5158.

(57) Giddings, J. C. *Dynamics of Chromatography, Part I, Principles and Theory*; Marcel Dekker: New York, 1965.